DALTON
FULL PAPER

Stereochemistry of nickel(II) complexes with *N*-glycosylamine ligands from 1,3-diaminopropane and aldopentoses. Correlation between configurational structures and circular dichroism spectra†

Tomoaki Tanase,* Yukiko Yasuda, Tomoko Onaka and Shigenobu Yano *

Department of Chemistry, Faculty of Science, Nara Women's University, Nara 630, Japan

Reactions of $[Ni(tn)_3]X_2{\cdot}2H_2O$ (tn = 1,3-diaminopropane, X = Cl or Br) with aldopentoses afforded a series of mononuclear nickel(II) complexes with *N*-glycosylamine ligands, $[Ni(aldose\text{-}tn)_2]X_2$ [aldose-tn = 1-(*N*-aldosyl)-amino-3-aminopropane, aldose = D-xylose (D-Xyl) **1**, D-lyxose (D-Lyx) **2**, D-ribose (D-Rib) **3**, or D-arabinose (D-Ara) **4**], which were characterized by elemental analysis, electronic absorption and circular dichroism (CD) spectroscopy, and X-ray crystallography. Compound **4b**, $[Ni(D\text{-}Ara\text{-}tn)_2]Br_2{\cdot}2H_2O$, was shown by an X-ray analysis to have a C_2 symmetrical mononuclear nickel(II) structure ligated by two tridentate *N*-glycosylamine ligands, 1-amino-3-(*N*-D-arabinosyl)propane. The two *N*-glycosylamines are co-ordinated to the metal through the primary amino and *N*-glycosidic secondary amino groups and the C-2 hydroxy group of the sugar moiety in a meridional mode, resulting in a Λ-C_2-helical configuration around the metal centre. The sugar rings adopt an unusual α-$^1C_4$ chair conformation and the sugar–chelate ring conformation is δ. The co-ordination behavior of D-ribose was confirmed by an X-ray analysis of an analogous compound, $[Ni(D\text{-}Rib\text{-}men)_2]Br_2{\cdot}2CH_3OH$ **5** [D-Rib-men = 1-methylamino-2-(*N*-D-ribosyl)aminoethane], derived from the reaction of $[Ni(men)_3]Br_2$ with D-ribose [men = 1-amino-2-(*N*-methylamino)ethane]. The D-ribose moiety forms an α-*N*-glycosidic bond with the primary amino group of men, and adopts an α-$^4C_1$ chair form, the sugar–chelate ring conformation being δ. The CD spectra of **1**–**4** were measured in the region 9000–50 000 cm^{-1} and clearly indicated the structural features of the complexes; the Cotton effects at around 10 000 cm^{-1} (the first absorption band of the d–d transitions) reflected the conformation of the sugar chelate or the absolute configuration of the *N*-glycosidic nitrogen atom, and those at around 40 000–46 000 cm^{-1} (charge-transfer bands) demonstrated the C_2 chiral configuration around the metal centre. These assignments were also confirmed by the CD spectra of known compounds.

The chemistry on interactions of metal ions with carbohydrates is of potential importance in the inorganic and bioinorganic fields, although the detailed stereochemistry of sugar–metal complexes is largely unexplored owing to the difficulty in isolating discrete compounds.[1–5]

We have systematically studied the syntheses and characterizations of complexes of Ni^{II},[6–28] Co^{II},[29–31] Co^{III},[32–35] Cu^{II},[36] and Mn^{II} [37,38] containing glycosylamines derived from the reactions between sugars and polyamines. Thermodynamically flexible and multifunctional carbohydrates could be assembled onto a metal centre through bond formation at the C-1 position of aldoses or the C-2 position of ketoses. For example, a ketohexose reacted with a diamine to form a *N*-glycosyldiamine which acted as a tetradentate ligand *via* the two oxygen atoms of the hydroxyl groups at the C-1 and C-3 positions and the two nitrogen atoms of the diamine.[8–10] Similarly, an aldohexose reacted with a diamine, *e.g.* 1,2-diaminoethane (en) or 1,3-diaminopropane (tn), to afford a *N*-aldosyl-en or -tn derivative which co-ordinated to a metal in a tridentate manner through the oxygen atom of the hydroxyl group at the C-2 position of the sugar moiety and the two nitrogen atoms of the diamine part.[6,7,12–14,23]

In the series of mononuclear nickel(II) complexes $[Ni(aldohexose\text{-}en)_2]X_2$ or $[Ni(aldohexose\text{-}tn)_2]X_2$ [aldohexose-en = 1-*N*-aldohexosylamino-2-aminoethane, aldohexose-tn = 1-*N*-aldohexosylamino-3-aminopropane; aldohexose = D-glucose (D-Glc), D-galactose (D-Gal), L-fucose (L-Fuc), D-mannose (D-Man), D-talose (D-Tal), L-rhamnose (6-deoxy-L-mannose) (L-Rha)] two tridentate *N*-aldosyldiamine ligands are co-ordinated in meridional mode to complete a *cis*(O,O)-$Ni(NNO)_2$ octahedron, in which all sugar moieties adopt

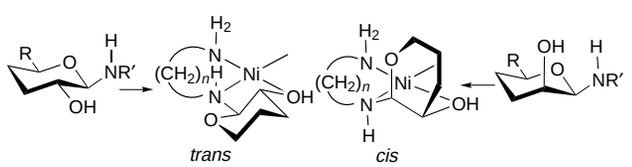

Scheme 1 R = CH_2OH, R′ = $(CH_2)_nNH_2$, n = 2 or 3

β-aldopyranosyl-$^4C_1$ structures. The co-ordination modes of the sugar parts are classified into two types denoted as the *trans*-chelation form of D-Glc, D-Gal, and L-Fuc and the *cis*-chelation form for D-Man, D-Tal, and L-Rha, on the basis of the crystal structure of $[Ni(L\text{-}Rha\text{-}tn)_2]Br_2{\cdot}2H_2O{\cdot}CH_3OH$ and their circular dichroism spectral patterns (Scheme 1).[14] In the *trans*-chelation form the sugar pyranoid ring is coplanar with the five-membered chelate ring whereas in the *cis*-chelation form, the sugar ring is considerably tilted with respect to the chelate ring.

Aldopentoses also participate in many biological systems, especially D-ribose derivatives in RNA and DNA backbones. Whereas systematic elucidation of the co-ordination behaviors of aldopentoses is of value, the nickel(II)-glycosylamine complexes from aldopentoses have not been isolated and characterized thus far. Aldopentoses, in general, show more flexible conformational structures in comparison with aldohexoses, mainly due to the absence of a C-6 hydroxymethyl group, which leads to complicated stereochemistry around a metal centre. In the present work, we have prepared a series of $[Ni(aldopentose\text{-}tn)_2]X_2$ (X = Cl or Br) complexes and determined by crystal structure of $[Ni(D\text{-}Ara\text{-}tn)_2]Br_2{\cdot}2H_2O$ (D-Ara = D-arabinose). Their stereostructures including the absolute configuration around the metal were revealed by the circular dichroism spectra in the first d–d transition and charge-transfer band regions.

† *Non-SI unit employed:* $\mu_B \approx 9.27 \times 10^{-24}$ J T^{-1}.

Experimental

Materials

All reagents were of the best commercial grade and were used as received. The complexes $[Ni(tn)_3]X_2\cdot 2H_2O$ (X = Cl or Br)[39] and $[Ni(men)_3]Br_2$[40] (men = *N*-methylethane-1,2-diamine) were prepared by the known methods. The following additional abbreviations are used: D-Xyl, D-xylose; D-Lyx, D-lyxose; D-Rib, D-ribose; D-GlcN, 2-amino-2-deoxy-D-glucose; aldose-tn, 1-*N*-aldosylamino-3-aminopropane; aldose-en, 1-*N*-aldosyl-2-amino-2-aminoethane.

Measurements

Electronic absorption spectra were recorded on a Shimadzu UV-3100 spectrometer and circular dichroism spectra on JASCO J-720/730 spectropolarimeters. Magnetic susceptibilities were measured at room temperature by the Evance method using a Sherwood Scientific Ltd. model MSB-MKI magnetic balance. Diamagnetic corrections were calculated from tables of Pascal's constants.[41] The IR spectra were measured on KBr pellets by using a JEOL FT/IR8300 spectrometer.

Preparation of complexes

$[Ni(D\text{-Xyl-tn})_2]Cl_2\cdot H_2O$ 1a·H_2O. A methanolic solution (100 cm^3) containing $[Ni(tn)_3]Cl_2\cdot 2H_2O$ (1.55 g, 4.0 mmol) and D-xylose (1.83 g, 12.2 mmol) was incubated at 64 °C for 10–15 min. The resultant dark blue solution was cooled to room temperature, concentrated to *ca.* 50 cm^3 by a rotary evaporator, and chromatographed on a Sephadex LH-20 gel permeation column (5 × 75 cm) eluted with methanol. The blue main band was collected and purified again by a Sephadex LH-20 GPC column (4 × 50 cm). The purified blue band was concentrated to ≈15 cm^3 and a small amount of propan-2-ol was added. The mixed-solvent solution was allowed to stand in a refrigerator for 2–3 d to yield blue microcrystals of complex **1a**·H_2O which were collected by a glass filter, washed with cold ethanol (≈2 cm^3) and diethyl ether (≈2 cm^3), and dried in vacuum (yield 18%, 403 mg) (Found: C, 33.99; H, 6.91; N, 9.89. Calc. for $C_{16}H_{38}Cl_2N_4NiO_9$: C, 34.31; H, 6.84; N, 10.00%).

$[Ni(D\text{-Xyl-tn})_2]Br_2\cdot CH_3OH$ 1b·CH_3OH. Complex **1b**·CH_3OH was prepared by a procedure similar to that for **1a**, using $[Ni(tn)_3]Br_2\cdot 2H_2O$ (1.96 g, 4.12 mmol) and D-xylose (1.85 g, 12.3 mmol) as starting materials. Yield 29% (782 mg) (Found: C, 30.79; H, 6.01; N, 8.68. Calc. for $C_{17}H_{40}Br_2N_4NiO_9$: C, 30.80; H, 6.08; N, 8.45%). μ_{eff} 3.09 μ_B.

$[Ni(D\text{-Lyx-tn})_2]Cl_2\cdot 1.5H_2O$ 2a·$1.5H_2O$. Complex **2a**·$1.5H_2O$ was prepared by a procedure similar to that for **1a**, using $[Ni(tn)_3]Cl_2\cdot 2H_2O$ (0.781 g, 2.01 mmol) and D-lyxose (0.941 g, 6.27 mmol) as starting materials. Yield 26% (298 mg). (Found: C, 33.58; H, 6.76; N, 9.16. Calc. for $C_{16}H_{39}Cl_2N_4NiO_{9.5}$: C, 33.77; H, 6.91; N, 9.84%).

$[Ni(D\text{-Lyx-tn})_2]Br_2\cdot CH_3OH$ 2b·CH_3OH. Complex **2b**·CH_3OH was prepared by a procedure similar to that for **1a**, using $[Ni(tn)_3]Br_2\cdot 2H_2O$ (0.893 g, 1.87 mmol) and D-lyxose (0.874 g, 5.82 mmol) as starting materials. The blue main fraction was concentrated to ≈8 cm^3 and ethanol (*ca.* 8 cm^3) was layered onto the solution, which was kept in a refrigerator for 2–3 d to afford blue microcrystals of **2b**·CH_3OH in 29% yield (357 mg) (Found: C, 30.61; H, 6.13; N, 8.80. Calc. for $C_{17}H_{40}Br_2N_4NiO_9$: C, 30.80; H, 6.08; N, 8.45%). μ_{eff} 3.03 μ_B.

$[Ni(D\text{-Rib-tn})_2]Cl_2\cdot CH_3OH\cdot H_2O$ 3a·CH_3OH·H_2O. Complex **3a**·CH_3OH·H_2O was prepared by a procedure similar to that for **1a**, using $[Ni(tn)_3]Cl_2\cdot 2H_2O$ (1.57 g, 4.05 mmol) and D-ribose (1.80 g, 12.0 mmol) as starting materials. The blue main band was concentrated to *ca.* 15 cm^3 and diethyl ether (4 cm^3) was added to the solution, which was kept in a refrigerator for 1–2 d to give blue microcrystals of **3a**·CH_3OH·H_2O in 19% yield (459 mg) (Found: C, 34.70; H, 7.25; N, 8.87. Calc. for $C_{17}H_{42}Cl_2N_4NiO_{10}$: C, 34.48; H, 7.15; N, 9.46%).

$[Ni(D\text{-Rib-tn})_2]Br_2\cdot H_2O$ 3b·H_2O. Complex **3b**·H_2O was prepared by a procedure similar to that for **1a**, using $[Ni(tn)_3]Br_2\cdot 2H_2O$ (1.90 g, 3.98 mmol) and D-ribose (1.80 g, 12.0 mmol) as starting materials. The blue main fraction was concentrated to ≈10 cm^3 and ethanol (*ca.* 10 cm^3) was layered onto the solution, which was kept in a refrigerator for 2–3 d to afford blue needle crystals of **3b**·H_2O in 24% yield (612 mg) (Found: C, 29.82; H, 6.25; N, 8.49. Calc. for $C_{16}H_{38}Br_2N_4NiO_9$: C, 29.61; H, 5.90; N, 8.63%). μ_{eff} 2.99 μ_B.

$[Ni(D\text{-Ara-tn})_2]Cl_2\cdot C_2H_5OH$ 4a·C_2H_5OH. Complex **4a**·C_2H_5OH was prepared by a procedure similar to that for **1a**, using $[Ni(tn)_3]Cl_2\cdot 2H_2O$ (1.55 g, 4.00 mmol) and D-arabinose (1.81 g, 12.0 mmol) as starting materials. Ethanol (10 cm^3) was layered onto the blue concentrated solution (10 cm^3), which was kept in a refrigerator for 2–3 d to afford blue needle crystals of **4a**·C_2H_5OH in 20% yield (459 mg) (Found: C, 36.46; H, 7.39; N, 10.04. Calc. for $C_{18}H_{42}Cl_2N_4NiO_9$: C, 36.76; H, 7.20; N, 9.53%).

$[Ni(D\text{-Ara-tn})_2]Br_2\cdot H_2O$ 4b·H_2O. Complex **4b**·H_2O was prepared by a procedure similar to that for **1a**, using $[Ni(tn)_3]Br_2\cdot 2H_2O$ (1.87 g, 3.93 mmol) and D-arabinose (1.79 g, 11.9 mmol) as starting materials. The blue main band was concentrated to *ca.* 15 cm^3 and a small amount of diethyl ether was slowly added. Then the solution was kept in a refrigerator for a week to yield blue prismatic crystals of **4b**·H_2O in 16% yield (412 mg) (Found: C, 29.81; H, 6.21; N, 8.56. Calc. for $C_{16}H_{38}Br_2N_4NiO_9$: C, 29.61; H, 5.90; N, 8.63%). μ_{eff} 2.96 μ_B.

$[Ni(D\text{-Rib-men})_2]Br_2\cdot H_2O$ 5·H_2O. Complex **5**·H_2O was prepared by a procedure similar to that for **1a**, using $[Ni(men)_3]Br_2$ (1.91 g, 4.33 mmol) and D-ribose (1.84 g, 12.2 mmol) as starting materials. The blue main band was collected and allowed to stand in a refrigerator for a week to yield blue prismatic crystals of **4b**·H_2O in 27% yield (752 mg) (Found: C, 29.99; H, 5.77; N, 8.76. Calc. for $C_{16}H_{38}Br_2N_4NiO_9$: C, 29.61; H, 5.90; N, 8.63%).

Crystallography

Careful crystallization of complexes **4b** and **5** from methanol and methanol–diethyl ether gave respective prismatic crystals of **4b**·$2H_2O$ and **5**·$2CH_3OH$, which were suitable for X-ray crystallography. Crystals used in the data collection were mounted on the end of a glass fiber with Paraton oil and the data collection was carried out at −100 °C on a Rigaku AFC7R diffractometer equipped with graphite-monochromated Mo-Kα (λ = 0.710 69 Å) radiation. Crystal data and experimental conditions are listed in Table 1. Three standard reflections were monitored every 150 and showed no systematic decrease in intensity. Reflection data were corrected for Lorentz-polarization effects and absorption corrections were applied by the ψ-scan method. The known absolute configurations of the sugar moieties were used as internal reference asymmetric centres to determine the space group $P6_122$ *vs.* $P6_522$ for **4a**·$2H_2O$ and $P4_12_12$ *vs.* $P4_32_12$ for **5**·$2CH_3OH$.

The structure of complex **4b**·$2H_2O$ was solved by direct methods with SIR 92.[42] Half of the complex cation, a bromide anion, and one solvent water were determined and the nickel atom sits in a special position with 0.5 occupancy. The majority of the non-hydrogen atoms were located initially and subsequent Fourier-difference syntheses gave the remainder. The C–H and N–H hydrogen atoms were located at ideal positions with a distance of 0.95 Å and not refined. The structure was refined with full-matrix least-squares techniques minimizing $\Sigma w(|F_o| - |F_c|)^2$. The Br anion was refined with a disordered

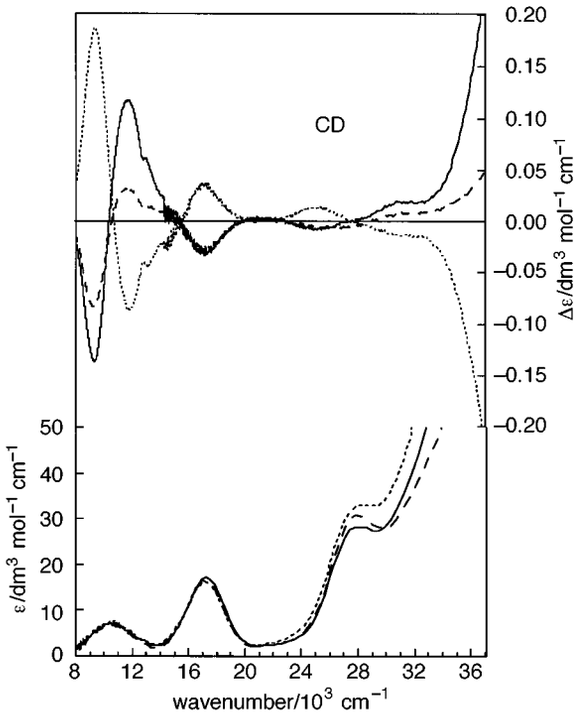

Fig. 1 Electronic absorption and circular dichroism spectra of $[Ni(D\text{-Xyl-tn})_2]Br_2$ **1b** (·····), $[Ni(D\text{-Lyx-tn})_2]Br_2$ **2b** (– – –), and $[Ni(D\text{-Ara-tn})_2]Br_2$ **4b** (——) in methanol in the d–d transition band region (8000–35 000 cm^{-1})

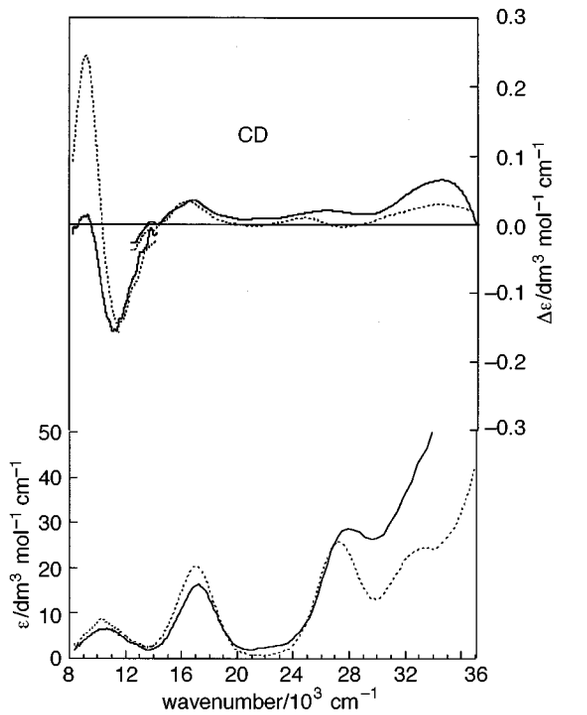

Fig. 2 Electronic absorption and circular dichroism spectra of $[Ni(D\text{-Rib-tn})_2]Br_2$ **3b** (——) and $[Ni(L\text{-Rha-tn})_2]Br_2$ **6** (– – –) in methanol in d–d transition band region

model involving three Br atoms having 0.5, 0.3, and 0.2 occupancies. Final refinement with anisotropic thermal parameters for all non-hydrogen atoms converged at $R = 0.085$ and $R' = 0.084$, where $R = \Sigma||F_o| - |F_c||/\Sigma|F_o|$ and $R' = [\Sigma w(|F_o| - |F_c|)^2/\Sigma w|F_o|^2]^{\frac{1}{2}}$ [$w = 1/\sigma^2(F_o)$]. The structure of **5**.$2CH_3OH$ was solved by direct methods with SIR 92 as for **4b**. The C–H and N–H hydrogen atoms except those of CH_3OH were located at ideal positions and the structure refined as for **4b** to $R = 0.060$ and $R' = 0.067$.

Atomic scattering factors and values of f' and f'' for Br, Ni, O, N, and C were taken from refs. 43 and 44. All calculations were carried out on a Silicon Graphics Indigo computer with the TEXSAN program package.[45]

CCDC reference number 186/797.

Results and Discussion

Preparation of $[Ni(N\text{-aldopentosyl-tn})_2]X_2$

Reactions of $[Ni(tn)_3]X_2{\cdot}2H_2O$ with D-aldopentoses in refluxing methanol afforded a series of nickel(II) complexes with *N*-aldopentosyl-1,3-diaminopropane ligands, $[Ni(aldose\text{-}tn)_2]X_2$ [aldose = D-Xyl **1**, D-Lyx **2**, D-Rib **3**, or D-Ara **4**; X = Cl **a** or Br **b**]. The isolated yields (16–29%) are considerably lower than those for the corresponding aldohexose complexes (40–85%).[14] The elemental analyses indicated that the complexes consisted of two glycosylamine ligands formed from an aldose and tn and two halide anions per metal. The magnetic moments of **1b**–**4b** (2.96–3.09 μ_B) indicated that the nickel(II) ions have two unpaired electrons in octahedral geometry.[46] Electronic absorption and circular dichroism (CD) spectra are shown in Figs. 1 and 2,‡ and representative spectral data are summarized in Table 1. The absorption spectral patterns, consisting of three principal bands with relatively low absorption coefficients, and the positions of the maxima, 10 400–10 800, 16 900–17 300 and 27 900–28 600 cm^{-1}, are closely similar to each other and are also comparable to those of $[Ni(N\text{-aldohexosyl-tn})_2]X_2$ having *cis*-(O,O)-$Ni^{II}N_4O_2$ octahedral structure.[14] The band maximum energy observed in the transmittance spectra were almost identical to those of the solution spectra. In the CD spectra distinct Cotton effects are observed in the range of d–d transitions, 9000–30 000 cm^{-1}, together with large effects in the charge-transfer band region, 35 000–45 000 cm^{-1}, clearly indicating co-ordination of the sugar parts to the metal centre. The *N*-glycosylamine formation between aldopentose and tn was evident in the IR spectra, in which the δ(N–H) band was broad and shifted to high energy compared with that of the diamine complex $[Ni(tn)_3]X_2{\cdot}2H_2O$. These analytical, magnetic, and spectral data strongly suggested that the structure of the first co-ordination sphere for **1**–**4** is identical to that of $[Ni(aldohexose\text{-}tn)_2]X_2$, namely octahedral *cis*-(O,O)-$Ni^{II}N_4O_2$ comprising two tridentate *N*-glycosylamine ligands, aldopentose-tn, in meridional mode.

‡ The absorption and CD spectra of the chloride complexes **1a**–**4a** were closely similar to those of the corresponding bromide complexes **1b**–**4b**.

Crystal structure of $[Ni(D\text{-Ara-tn})_2]Br_2{\cdot}2H_2O$ **4b**·$2H_2O$

An ORTEP[47] diagram of the cation of complex **4b**·$2H_2O$ with the atomic numbering scheme is given in Fig. 3(*a*) and selected bond lengths and angles are listed in Table 3. The complex cation has a crystallographically imposed C_2 symmetry and consists of a nickel(II) ion ligated by two *N*-D-arabinosyl-tn ligands, D-Ara-tn, resulting in a *cis*-(O,O)-NiN_4O_2 octahedral geometry. The complex cation is fairly distorted from ideal O_h symmetry with the minimum *trans* angle of 170.1(3)° [O(2)–Ni–N(2)] and the minimum *cis* angle of 80.0(3)° [O(2)–Ni–N(1)], as observed in $[Ni(L\text{-Rha-tn})_2]^{2+}$ **6** and $[Ni(Mal\text{-tn})_2]^{2+}$ **7**[23] [Mal = maltose, *i.e.* (α-D-glycopyranosyl-(1→4)-D-glucose]. The two D-Ara-tn ligands bind to the metal in meridional fashion through the two amino nitrogen atoms [Ni–N(1) 2.143(8), Ni–N(2) 2.03(1) Å] and the C-2 hydroxy oxygen atom [Ni–O(2) 2.145(8) Å]. The absolute configuration (C_2 helical configuration) is Λ as shown in Fig. 3(*b*). The two possible configurations around the metal are depicted in Fig. 4. There seems to be no significant difference between them because the two sugar units are apart from each other in both configurations, but the Δ structure might be somewhat destabilized by a

Table 1 Electronic absorption, circular dichroism (CD), and transmittance spectral data

Complex	Absorption[a] $10^{-3}\ \tilde{\nu}_{max}/cm^{-1}$ ($\varepsilon/dm^3\ mol^{-1}\ cm^{-1}$)	CD[a] $10^{-3}\ \tilde{\nu}_{max}/cm^{-1}$ ($10^{-2}\ \Delta\varepsilon/dm^3\ mol^{-1}\ cm^{-1}$)	Transmittance[b] $10^{-3}\ \tilde{\nu}_{max}/cm^{-1}$
[Ni(D-Xyl-tn)$_2$]$Br_2\cdot CH_3OH$	10.5(7.5)	9.4(+18.7)	10.5
1b$\cdot CH_3OH$		11.7(−8.7)	
	17.2(16.3)	17.0(+3.8)	17.2
		20.7(−0.2)	
	28.3 (sh)(32.2)	25.3(+1.4)	28.1 (sh)
		44.3(−164)	
[Ni(D-Lyx-tn)$_2$]$Br_2\cdot CH_3OH$	10.4(6.9)	9.2(−8.3)	10.7
2b$\cdot CH_3OH$		11.7(+3.4)	
	17.2(16.7)	17.1(−3.1)	17.3
		20.8(+0.3)	
	27.9(31.1)	26.8(−0.7)	27.8 (sh)
		30.2(+1.9)	
		35.1(+2.6)	
		43.9(+64.0)	
[Ni(D-Rib-tn)$_2$]$Br_2\cdot H_2O$	10.7(6.8)	9.3(+3.5)	10.5
3b$\cdot H_2O$		11.3(−11.5)	
	17.2(16.5)	17.4(+2.7)	17.3
		21.3(−0.3)	
	27.9(28.9)	29.1(+1.0)	
		33.6(+3.2)	27.8 (sh)
		44.3(−153)	
[Ni(D)-Ara-tn]$_2Br_2\cdot H_2O$	10.4(7.1)	9.3(−13.7)	10.5
4b$\cdot H_2O$		11.8(+11.8)	
	17.3(17.3)	17.1(−3.3)	17.3
		20.9(+0.5)	
	27.9(28.6)	25.4(−0.8)	27.9 (sh)
		30.7(+5.5)	
		35.6(+5.0)	
		43.9(+277)	
[Ni(D-Xyl-tn)$_2$]$Cl_2\cdot H_2O$	10.4(4.4)	9.3(+13.1)	10.5
1a$\cdot H_2O$		11.5(−11.0)	
	16.9(9.6)	16.6(+3.3)	17.0
		20.6(−0.1)	
	28.1 (sh)(30.0)	25.0(+1.7)	27.6 (sh)
[Ni(D-Lyx-tn)$_2$]$Cl_2\cdot 1.5H_2O$	10.8(4.5)	9.1(−6.7)	10.8
2a$\cdot 1.5H_2O$		11.6(+5.0)	
	17.2(9.5)	16.8(−1.6)	17.4
		21.5(+0.6)	
	27.9(18.1)	24.9(−0.1)	27.8 (sh)
		29.9(+1.4)	
		44.1(+50.8)	
[Ni(D-Rib-tn)$_2$]$Cl_2\cdot CH_3OH\cdot H_2O$	10.7(4.0)	9.1(+1.0)	10.6
3a$\cdot CH_3OH\cdot H_2O$		11.3(−12.8)	
	17.2(12.1)	16.8(+2.5)	17.2
		21.2(+0.2)	
	28.1(21.4)	26.3(+1.5)	28.1 (sh)
		34.1(+4.0)	
		43.9(−100)	
[Ni(D-Ara-tn)$_2$]$Cl_2\cdot C_2H_5OH$	10.4(4.4)	9.1(−5.6)	10.4
4a$\cdot C_2H_5OH$		11.2(+17.4)	
	17.1(12.1)	16.5(−2.4)	17.3
		21.2(+0.5)	
	28.6(21.7)	25.1(−0.6)	28.7 (sh)
		30.8(+2.9)	
		43.7(+250)	
[Ni(D-Rib-men)$_2$]$Br_2\cdot H_2O$	10.3(10.3)	10.7(+8.1)	10.5
5$\cdot H_2O$		15.5(−2.9)	
	17.0(12.3)	18.4(+5.2)	17.1
		22.4(+0.4)	
	28.4(43.9)	25.8(+2.1)	28.4 (sh)
		29.9(−0.3)	

[a] In methanol. [b] Nujol mull.

repulsive interaction between the two axially oriented NH protons of the primary amino groups. The most salient feature is that the sugar units adopt an unusual α-$^1C_4$-chair pyranoid conformation. This is the first example of metal–*N*-glycosamine complexes in which an aldose binds to an amino group through an α-*N*-glycosidic linkage. The α-$^1C_4$-chair structure is, however, the most thermodynamically stable in the free state of D-arabinose. The sugar co-ordination mode is *trans* (Scheme 1) and the *gauche* conformation of the sugar chelate ring NiN(1)C(1)C(2)O(2) is δ. The absolute configuration of the *N*-glycosidic nitrogen atoms N(1) is *R*. These structural parameters are abbreviated as Λ-(*trans*-δ-)-*R*-(α-$^1C_4$) in the present paper. The six-membered chelate ring NiN(1)C(6)C(7)C(8)N(2) adopts a stable chair conformation with a bite angle of 92.0(4)° [N(1)–Ni–N(2)], just like complexes **6** and **7**.

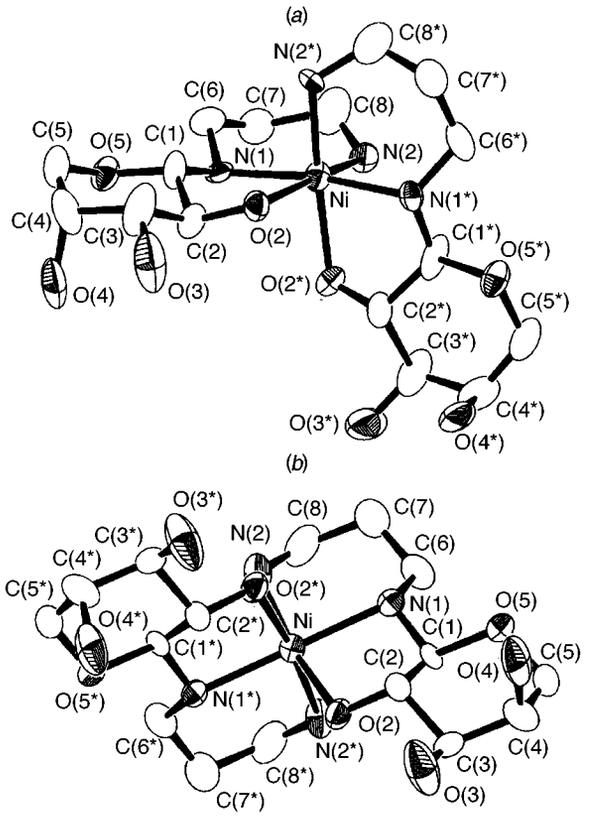

Fig. 3 An ORTEP plot (*a*) of the complex cation of [Ni(D-Ara-tn)$_2$]-Br_2·2H_2O **4b**·2H_2O, (*b*) viewed along C_2 axis

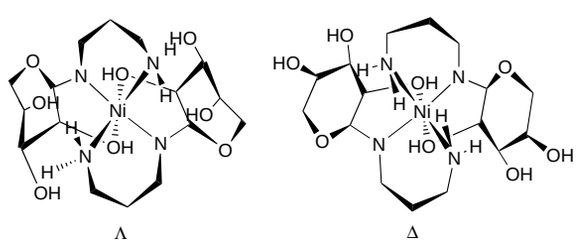

Fig. 4 Two possible C_2 helical configurations, Δ and Λ, for [Ni(D-Ara-tn)$_2$]$^{2+}$ **4**

Correlation between stereostructures and circular dichroism spectra

In general the D-arabinosylamine moiety in the pyranose form is able to chelate to a metal in three different modes, (*cis*-δ)-(β-$^4C_1$), (*trans*-δ)-(α-$^1C_4$), and (*cis*-λ)-(β-$^1C_4$), as shown in Fig. 5. The α-$^4C_1$ form is not suitable for chelation. In these structures, the α-$^1C_4$ form is seemingly the most thermodynamically stable and, in fact, the (*trans*-δ)-*R*-(α-$^1C_4$) mode is observed in the crystal structure of complex **4b**. The CD spectral features are in good accord with the crystal structure (Fig. 1). The spectral pattern could be classified as a *trans*-chelation type and the sign of the Cotton effect around the first d–d transition band (8000–14 000 cm^{-1}) varied from (−) to (+) with increasing wavenumber, suggesting that the sugar–chelate ring conformation is δ and the absolute configuration of the *N*-glycosidic nitrogen atom is *R*. The absolute configuration of the *N*-glycosidic N atom depends on the conformation of the sugar–chelate ring in the event that the six-membered diamine chelate ring adopts a stable chair conformation.

The CD spectral patterns of complexes **1b** (D-Xyl) and **2b** (D-Lyx) are also characteristic of the *trans*-sugar-chelation type (Fig. 1); that of **2b** is closely similar to that of **4b** and that of **1a** is a mirror image of the spectrum of **4b**. These clearly indicated the (*trans*-λ)-*S*-(β-$^4C_1$-D-Xyl) structure in **1b** and (*trans*-δ)-*R*-(α-$^1C_4$-D-Lyx) in **2b**. The structural parameters are summarized in Table 4. It should be noted that although the β-D-xylopyranose-$^4C_1$ structure is significantly more stable than the α-$^4C_1$ and α-$^1C_4$ forms, the thermodynamic stability of α-D-lyxopyranose-$^1C_4$ should be comparable to that of the β-$^4C_1$ form.

As to the D-ribose complex **3b**, the CD spectrum could be recognized as of a *cis*-sugar-chelation type, and is, indeed, quite similar to that of [Ni(L-Rha-tn)$_2$]Br_2 **6** which has a *cis*-λ sugar chelation (Fig. 2).[14] On the basis of the spectral data,

Table 2 Crystallographic and experimental data for [Ni(D-Ara-tn)$_2$]-Br_2·2H_2O **4b**·2H_2O and [Ni(D-Rib-men)$_2$]Br_2·2CH_3OH **5**·2CH_3OH

	4b·2H_2O	**5**·2CH_3OH
Formula	$C_{16}H_{40}Br_2N_4NiO_{10}$	$C_{18}H_{44}Br_2N_4NiO_{10}$
M	667.02	695.07
Crystal system	Hexagonal	Tetragonal
Space group	$P6_122$ (no. 178)	$P4_12_12$ (no. 92)
a/Å	22.288(7)	8.918(3)
c/Å	13.309(5)	35.588(11)
U/Å^3	5725(2)	2830(1)
Z	6	4
D_c/g cm^{-3}	1.161	1.631
μ/cm^{-1}	26.45	35.71
2θ Range/°	3–50	3–50
No. unique data	1983	1580
No. observed data	877	1275
	[$I > 2.5\sigma(I)$]	[$I > 3\sigma(I)$]
No. variables	163	160
R	0.085	0.060
R′	0.084	0.067

Table 3 Selected bond distances (Å) and angles (°) for [Ni(D-Ara-tn)$_2$]-Br_2·2H_2O **4b**·2H_2O with estimated standard deviations (e.s.d.s) in parentheses

Ni–O(2)	2.145(8)	Ni–N(1)	2.143(8)
Ni–N(2)	2.03(1)	O(2)–C(2)	1.37(1)
O(3)–C(3)	1.38(2)	O(4)–C(4)	1.55(2)
O(5)–C(1)	1.45(1)	O(5)–C(5)	1.46(2)
N(1)–C(1)	1.43(2)	N(1)–C(6)	1.45(2)
N(2)–C(8)	1.43(2)	C(1)–C(2)	1.49(2)
C(2)–C(3)	1.58(2)	C(3)–C(4)	1.52(2)
C(4)–C(5)	1.41(2)	C(6)–C(7)	1.49(2)
C(7)–C(8)	1.58(2)		
O(2)–Ni–O(2*)	88.9(4)	O(2)–Ni–N(1)	80.0(3)
O(2)–Ni–N(1*)	93.2(3)	O(2)–Ni–N(2)	170.1(3)
O(2)–Ni–N(2*)	85.7(3)	N(1)–Ni–N(1*)	170.6(5)
N(1)–Ni–N(2)	92.0(4)	N(1)–Ni–N(2*)	94.0(3)
N(2)–Ni–N(2*)	100.9(5)	Ni–O(2)–C(2)	111.0(7)
Ni–N(1)–C(1)	103.2(7)	Ni–N(1)–C(6)	117.9(7)
Ni–N(2)–C(8)	118.1(9)		

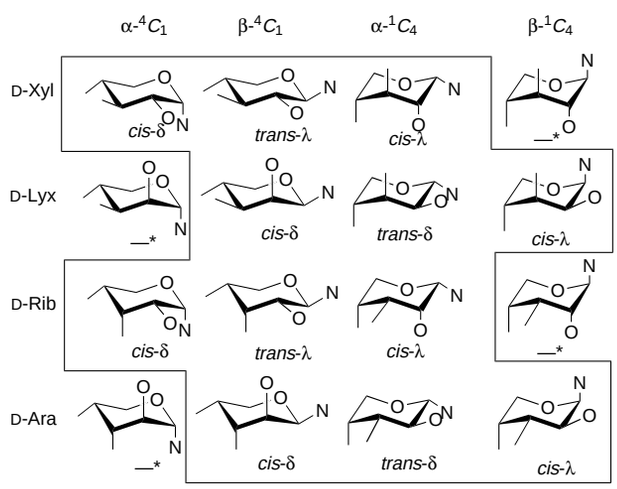

Fig. 5 Sugar pyranoid conformations which are able to chelate to a metal center

Table 4 Structural parameters for C_2 symmetrical nickel(II) complexes containing two tridentate *N*-glycosylamine ligands

Complex	Absolute configuration around metal	Sugar chelation and its conformation	Configuration of *N*-glycosidic N atom	Sugar pyranoid conformation
6 [Ni(L-Rha-tn)$_2$]Br$_2$ [a]	Δ	*cis*-λ	*S*	β-$^4C_1$
7 [Ni(Mal-tn)$_2$]Cl$_2$ [a]	Δ	*trans*-λ	*S*	β-$^4C_1$ [b]
8 [Ni(D-GlcN-tn)$_2$]Cl$_2$ [a]	Δ	*trans*-λ	*S*	β-$^4C_1$
9 [Ni(D-GlcN-en)$_2$]Cl$_2$ [a]	Λ	*trans*-λ	*S*	β-$^4C_1$
4b [Ni(D-Ara-tn)$_2$]Br$_2$ [a]	Λ	*trans*-δ	*R*	α-$^1C_4$
1 [Ni(D-Xyl-tn)$_2$]$^{2+}$	Δ	*trans*-λ	*S*	β-$^4C_1$
2 [Ni(D-Lyx-tn)$_2$]$^{2+}$	Λ	*trans*-δ	*R*	α-$^1C_4$
3 [Ni(D-Rib-tn)$_2$]$^{2+}$	Δ	*cis*-λ	*S*	α-$^1C_4$
5 [Ni(D-Rib-men)$_2$]Br$_2$ [a]	Δ	*cis*-δ	*R*	α-$^4C_1$

[a] Determined by X-ray crystallography. [b] Structure for the reducing terminal sugar, the chelating sugar.

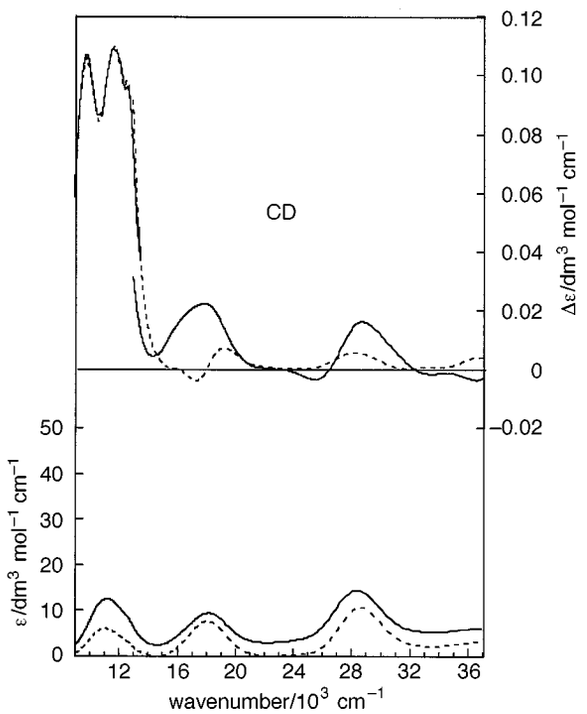

Fig. 6 Electronic absorption and circular dichroism spectra of [Ni(D-GlcN-tn)$_2$]Cl$_2$ **8** (----) and [Ni(D-GlcN-en)$_2$]Cl$_2$ **9** (——) in methanol

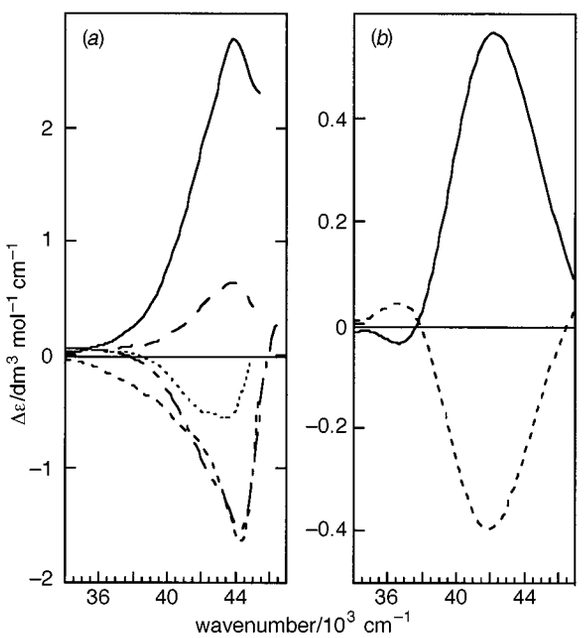

Fig. 7 Circular dichroism spectra in the charge-transfer band region in methanol. (*a*) [Ni(D-Xyl-tn)$_2$]Br$_2$ **1b** (-----), [Ni(D-Lyx-tn)$_2$]Br$_2$ **2b** (——), [Ni(D-Rib-tn)$_2$]Br$_2$ **3b** (— — —), [Ni(D-Ara-tn)$_2$]Br$_2$ **4b** (——) and [Ni(L-Rha-tn)$_2$]Br$_2$ **6** (– – –); (*b*) [Ni(D-GlcN-en)$_2$]Cl$_2$ **8** (——) and [Ni(D-GlcN-tn)$_2$]Cl$_2$ (------)

complex **3b** is assumed to contain a (*cis*-λ)-*S*-(α-$^1C_4$-D-Rib) structure, although the α-$^1C_4$ form is rather thermodynamically unfavored among the three possible structures indicated in Fig. 5. It is not clear at present why the sugar part does not adopt the most favorable (*trans*-λ) chelation form with the β-pyranose-$^4C_1$ structure.

The arrangement of two meridional NNO ligands generates a C_2 chirality at the metal centre as depicted in Fig. 4, but we have not discussed the definite absolute configuration (Δ or Λ) around the metal centre of nickel aldohexosyl diamine complexes thus far because it was not clearly correlated to the CD spectral pattern in the region of 9000–35 000 cm^{-1}. In this work we have carefully measured the CD spectra not only in the d–d transition region (8000–35 000 cm^{-1}) but in the charge-transfer band area (35 000–45 000 cm^{-1}), and have newly found that the sign of Cotton effect in the latter region exclusively reflects the absolute configuration around the metal centre from a compilation of crystal structures and CD spectra of analogous compounds which are listed in Table 4. For example, the CD spectra of [Ni(D-GlcN-tn)$_2$]$^{2+}$ **8**[28] and [Ni(D-GlcN-en)$_2$]$^{2+}$ **9**[12] are shown in Figs. 6 and 7(*b*). The structures of complexes **8** and **9** were determined by X-ray crystallography to be Δ-(*trans*-λ)-*S*-(β-$^4C_1$-D-GlcN) and Λ-(*trans*-λ)-*S*-(β-$^4C_1$-D-GlcN), respectively (Fig. 8); the absolute configurations around the metal centre are opposite to each other in spite of the fact that the local structures of the sugar moiety are identical, (*trans*-λ)-*S*-(β-$^4C_1$-D-GlcN). Their CD spectral patterns in the region 9000–15 000 cm^{-1} are almost identical (Fig. 6) and those at 35 000–45 000 cm^{-1} are mirror images [Fig. 7(*b*)], strongly suggesting that the CD spectra reflect the sugar-chelation structure in the first d–d transition band and the C_2 chiral configuration around the metal in the charge-transfer region (35 000–45 000 cm^{-1}) independently. The (+) sign at about 40 000 cm^{-1} corresponds to the Λ configuration and the (−) sign to the Δ. This empirical rule is also consistent with the CD spectral sign at around 40 000 cm^{-1} for the structurally characterized complexes **6**, **7**, and **4a** (Table 4). In the light of this sign, **1** (D-Xyl), **2** (D-Lyx), and **3** (D-Rib) were assumed to have C_2 chiral configurations around the metal of Δ, Λ, and Δ, respectively (Table 4 and Fig. 9). On the basis of the CD spectral signs, the C_2 chiral absolute configurations of [Ni(D-Glc-tn)$_2$]$^{2+}$ and [Ni(D-Gal-tn)$_2$]$^{2+}$ reported in ref. 14 were reassigned as Δ.

Crystal structure of [Ni(D-Rib-men)$_2$]Br$_2$·2CH$_3$OH 5·2CH$_3$OH

Although furanose forms of aldopentoses are extremely unstable in comparison with pyranose forms in the free states, some attempts to confirm the D-ribopyranosyl structure have been made because the α-D-ribofuranoside moiety involves a

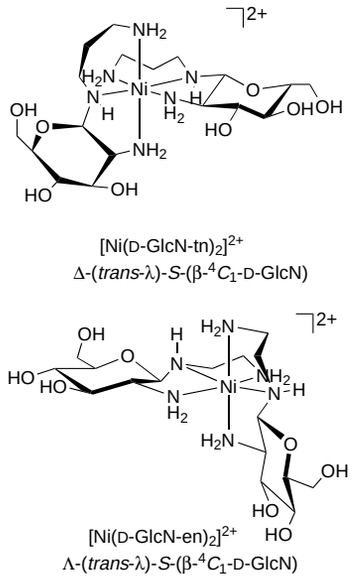

Fig. 8 Structures of the complex cations of $[Ni(D\text{-}GlcN\text{-}tn)_2]Cl_2$ **8** and $[Ni(D\text{-}GlcN\text{-}en)_2]Cl_2$ **9** determined by X-ray crystallography

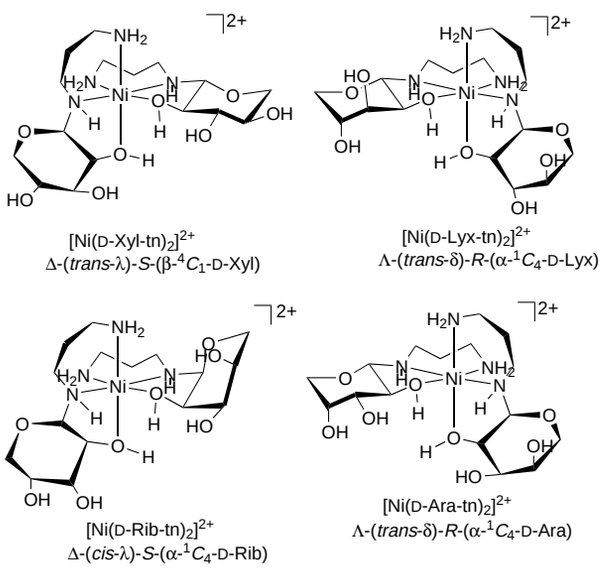

Fig. 9 Stereostructures of the cations of nickel aldopentosyldiamine complexes

cis,*cis* sequence of three donor atoms which was known to possess high affinity for a metal centre. Whereas good crystals of complex **3** were not obtained, replacing tn by men led to successful isolation of single crystals of $[Ni(D\text{-}Rib\text{-}men)_2]Br_2\cdot 2CH_3OH$ **5**·$2CH_3OH$. It should be noted that complex **5** is very unstable even in the solid state and its CD spectrum is entirely different from that of **3**. The diamine part may significantly influence the stereostructure. An ORTEP plot of the complex cation with the atomic numbering scheme is shown in Fig. 10, and bond lengths and angles around the nickel are listed in Table 5. The structure involves a *cis*-(O,O)-NiN_4O_2 octahedral core similar to that found in **3b**. Two D-ribose molecules are anchored onto the metal as an α-*N*-pyranoside structure, forming a *cis* chelation with a δ *gauche* conformation through the *C*-2 hydroxy oxygen and the *N*-glycosidic nitrogen atoms. The absolute configuration around the metal centre is Δ and that of N(1) is *R*. The men part also chelates with a λ *gauche* form of the five-membered ring, the methyl group on N(2) being equatorially directed.

Conclusion

A new series of C_2 symmetrical nickel(II) complexes containing two tridentate *N*-glycosylamine ligands from 1,3-diaminopropane and aldopentoses, $[Ni(aldopentose\text{-}tn)_2]^{2+}$, was successfully synthesized and their stereostructures, the C_2 chiral configuration around the metal, sugar conformation and its anomeric form, conformation of the sugar chelation, and the absolute configuration of the *N*-glycosidic nitrogen, were systematically determined by X-ray crystallography and CD spectroscopy as shown in Fig. 9. It was newly found that the sign of the Cotton effect at around 40 000 cm^{-1} exclusively correlates to the absolute configuration around the metal centre. The aldopentoses showed more flexible behavior than aldohexoses owing to the absence of a C-6 substituent group; both α- and β-anomeric forms and $^4C_1$- and $^1C_4$-pyranoid conformations were observed, probably to release steric repulsive interactions around the metal centre as well as in the sugar parts. The present results could provide useful insights into the detailed stereochemistry of metal–sugar complexes.

Table 5 Selected bond distances (Å) and angles (°) for $[Ni(D\text{-}Rib\text{-}men)_2]Br_2\cdot 2CH_3OH$ **5**·$2CH_3OH$ with e.s.d.s in parentheses

Ni–O(2)	2.169(7)	Ni–N(1)	2.070(9)
Ni–N(2)	2.097(9)	O(2)–C(2)	1.45(1)
O(3)–C(3)	1.42(1)	O(4)–C(4)	1.42(1)
O(5)–C(1)	1.39(1)	O(5)–C(5)	1.46(1)
N(1)–C(1)	1.46(1)	N(1)–C(6)	1.44(1)
N(2)–C(7)	1.47(1)	N(2)–C(8)	1.43(2)
C(1)–C(2)	1.57(2)	C(2)–C(3)	1.50(1)
C(3)–C(4)	1.53(2)	C(4)–C(5)	1.49(2)
C(6)–C(7)	1.53(2)		
O(2)–Ni–O(2*)	85.5(4)	O(2)–Ni–N(1)	79.8(3)
O(2)–Ni–N(1*)	95.0(3)	O(2)–Ni–N(2)	161.2(3)
O(2)–Ni–N(2*)	86.5(3)	N(1)–Ni–N(1*)	173.0(5)
N(1)–Ni–N(2)	83.9(3)	N(1)–Ni–N(2*)	100.3(4)
N(2)–Ni–N(2*)	105.8(6)	Ni–O(2)–C(2)	112.1(6)
Ni–N(1)–C(1)	109.6(6)	Ni–N(1)–C(6)	106.9(6)
Ni–N(2)–C(7)	107.0(6)	Ni–N(2)–C(8)	122.7(8)

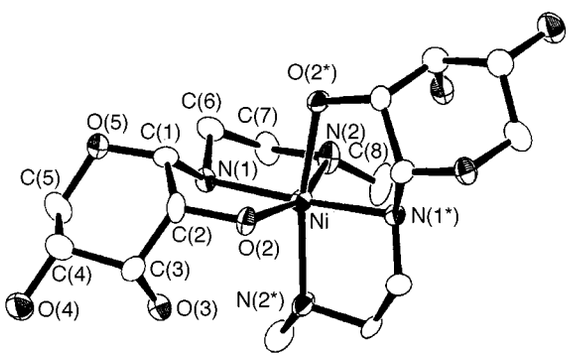

Fig. 10 An ORTEP diagram of the complex cation of $[Ni(D\text{-}Rib\text{-}men)_2]Br_2\cdot 2CH_3OH$ **5**·$2CH_3OH$

Acknowledgements

The authors thank Professors Ikuko Miyahara and Ken Hirotsu of Osaka City University for obtaining preliminary X-ray data for complex **4b**. This work was partially supported by a Grant-in-Aid for Scientific Research from the Ministry of Education of Japan and Grants from Iwatani, Nippon Itagarasu, Mitsubishi-Yuka, and Nagase Foundations and the San-Ei Gen Foundation for Food Chemical Research.

References

1 S. J. Angyal, *Chem. Soc. Rev.*, 1980, **9**, 415.
2 S. J. Angyal, *Adv. Carbohydr. Chem. Biochem.*, 1989, **47**, 1.
3 D. M. Whitfield, S. Stojkovski and B. Sarkar, *Coord. Chem. Rev.*, 1993, **122**, 171.
4 S. Yano, *Coord. Chem. Rev.*, 1988, **92**, 113.

5 S. Yano and K. Otsuka, *Metal Ions in Biological Systems*, Marcel Dekker, New York, 1996, p. 27.
6 S. Takizawa, H. Sugita, S. Yano and S. Yoshikawa, *J. Am. Chem. Soc.*, 1980, **102**, 7969.
7 S. Yano, S. Takizawa, H. Sugita, T. Takahashi, T. Tsubomura, H. Shioi and S. Yoshikawa, *Carbohydr. Res.*, 1985, **142**, 179.
8 T. Tsubomura, S. Yano, K. Toriumi, T. Ito and S. Yoshikawa, *Polyhedron*, 1983, **2**, 123.
9 T. Tsubomura, S. Yano, K. Toriumi, T. Ito and S. Yoshikawa, *Bull. Chem. Soc. Jpn.*, 1984, **57**, 1833.
10 T. Tsubomura, S. Yano, K. Toriumi, T. Ito and S. Yoshikawa, *Inorg. Chem.*, 1985, **24**, 3218.
11 T. Tsubomura, S. Yano and S. Yoshikawa, *Inorg. Chem.*, 1986, **25**, 392.
12 S. Yano, T. Sakai, K. Toriumi, T. Ito and S. Yoshikawa, *Inorg. Chem.*, 1985, **24**, 498.
13 H. Shioi, S. Yano, K. Toriumi, T. Ito and S. Yoshikawa, *J. Chem. Soc.*, *Chem. Commun.*, 1983, 201.
14 S. Yano, M. Kato, H. Shioi, T. Takahashi, T. Tsubomura, K. Toriumi, T. Ito, M. Hidai and S. Yoshikawa, *J. Chem. Soc.*, *Dalton Trans.*, 1993, 1699.
15 T. Tanase, K. Kurihara, S. Yano, K. Kobayashi, T. Sakurai and S. Yoshikawa, *J. Chem. Soc.*, *Chem. Commun.*, 1985, 1562.
16 T. Tanase, F. Shimizu, S. Yano and S. Yoshikawa, *J. Chem. Soc.*, *Chem. Commun.*, 1986, 1001.
17 T. Tanase, K. Kurihara, S. Yano, K. Kobayashi, T. Sakurai and S. Yoshikawa, *Inorg. Chem.*, 1987, **26**, 3134.
18 T. Tanase, T. Murata, S. Yano, M. Hidai and S. Yoshikawa, *Chem. Lett.*, 1987, 1409.
19 T. Tanase, F. Shimizu, K. Kuse, S. Yano, S. Yoshikawa and M. Hidai, *J. Chem. Soc.*, *Chem. Commun.*, 1987, 659.
20 T. Tanase, F. Shimizu, S. Yano, M. Hidai, S. Yoshikawa and K. Asakura, *J. Chem. Soc. Jpn.*, 1987, **3**, 322.
21 T. Tanase, K. Ishida, T. Watanabe, M. Komiyama, K. Koumoto, S. Yano, M. Hidai and S. Yoshikawa, *Chem. Lett.*, 1988, 327.
22 T. Tanase, F. Shimizu, M. Kuse, S. Yano, M. Hidai and S. Yoshikawa, *Inorg. Chem.*, 1988, **27**, 4085.
23 T. Tanase, R. Nouchi, Y. Oka, M. Kato, N. Nakamura, T. Yamamura, Y. Yamamoto and S. Yano, *J. Chem. Soc.*, *Dalton Trans.*, 1993, 2645.
24 T. Takei, T. Tanase, S. Yano and M. Hidai, *Chem. Lett.*, 1991, 1629.
25 S. Yano, T. Takahashi, Y. Sato, K. Ishida, T. Tanase, M. Hidai, K. Kobayashi and T. Sakurai, *Chem. Lett.*, 1987, 2153.
26 S. Yano, M. Doi, M. Kato, I. Okura, T. Nagano, Y. Yamamoto and T. Tanase, *Inorg. Chim. Acta*, 1996, **249**, 1.
27 T. Tanase, R. N. M. Doi, M. Kato, Y. Sato, K. Ishida, K. Kobayashi, T. Sakurai, Y. Yamamoto and S. Yano, *Inorg. Chem.*, 1996, **35**, 4848.
28 S. Yano, S. Inoue, R. Nouchi, K. Mogami, Y. Shinohara, Y. Yasuda, M. Kato, T. Tanase, T. Kakuchi, Y. Mikata, T. Suzuki and Y. Yamamoto, *J. Inorg. Biochem.*, in the press.
29 T. Tanase, M. Nakagoshi, A. Teratani, M. Kato, Y. Yamamoto and S. Yano, *Inorg. Chem.*, 1994, **33**, 6.
30 S. Yano, M. Nakagoshi, A. Tertani, M. Kato, T. Tanase, Y. Yamamoto, H. Uekusa and Y. Ohashi, *Mol. Cryst. Liq. Cryst.*, 1996, **276**, 253.
31 S. Yano, M. Nakagoshi, A. Teratani, M. Kato, T. Onaka, M. Iida, T. Tanase, Y. Yamamoto, H. Uekusa and Y. Ohashi, *Inorg. Chem.*, 1997, **36**, 4187.
32 K. Ishida, S. Yano and S. Yoshikawa, *Inorg. Chem.*, 1986, **25**, 3552.
33 K. Ishida, M. Yashiro, S. Yano, M. Hidai and S. Yoshikawa, *J. Am. Chem. Soc.*, 1988, **110**, 2015.
34 K. Ishida, S. Nonoyama, T. Hirano, S. Yano, M.Hidai and S. Yoshikawa, *J. Am. Chem. Soc.*, 1989, **111**, 1599.
35 K. Ishida, M. Yashiro, S. Yano, M. Hidai and S. Yoshikawa, *J. Chem. Soc.*, *Dalton Trans.*, 1989, 1241.
36 T. Tanase, K. Mano and Y. Yamamoto, *Inorg. Chem.*, 1993, **32**, 3995.
37 S. Yano, S. T. M. Doi, W. Mori, M. Mikuriya, A. Ichimura, I. Kinoshita, Y. Yamamoto and T. Tanase, *Chem. Commun.*, 1997, 997.
38 T. Tanase, S. Tamakoshi, M. Doi, W. Mori and S. Yano, *Inorg. Chim. Acta*, 1997, **266**, 5.
39 D. A. House and N. F. Curtis, *J. Am. Chem. Soc.*, 1964, **86**, 223.
40 R. N. Keller and L. J. Edwards, *J. Am. Chem. Soc.*, 1952, **74**, 215.
41 B. N. Figgis and J. Lewis, *Modern Coordination Chemistry*, Interscience, New York, 1960, p. 403.
42 M. C. Burla, M. Camalli, G. Cascarano, C. Giacovazzo, G. Polidori, R. Spagna and D. Viterbo, *J. Appl. Crystallogr.*, 1989, **22**, 389.
43 D. T. Cromer, *Acta Crystallogr.*, 1965, **18**, 17.
44 D. T. Cromer and J. T. Waber, *International Tables for X-Ray Crystallography*, Kynoch Press, Birmingham, 1974.
45 TEXSAN Structure Analysis Package, Molecular Structure Corporation, The Woodlands, TX, 1985.
46 F. A. Cotton and G. Wilkinson, *Advanced Inorganic Chemistry*, Interscience, New York, 1972.
47 C. K. Johnson, ORTEP, Report ORNL-5138, Oak Ridge National Laboratory, Oak Ridge, TN, 1976.

Received 15*th September* 1997; *Paper* 7/06676G